JACS
JOURNAL OF THE AMERICAN CHEMICAL SOCIETY
Communication
pubs.acs.org/JACS

Why Can Hydrogen Sulfide Permeate Cell Membranes?

Saleh Riahi and Christopher N. Rowley*

Department of Chemistry, Memorial University of Newfoundland, St. John's, Newfoundland A1B 3X7, Canada

Supporting Information

ABSTRACT: The high membrane permeability of H_2S was studied using polarizable molecular dynamics simulations of a DPPC lipid bilayer. The solubility–diffusion model predicts permeability coefficients of H_2S and H_2O that are in good agreement with experiment. The computed diffusion coefficient profile shows H_2S to diffuse at a lower rate than H_2O, but the barrier for H_2S permeation on the Gibbs energy profile is negligible. The hydrophobicity of H_2S allows it to partition into the paraffinic interior of the membrane readily.

Hydrogen sulfide (H_2S) is an exceptionally toxic gas, with a recommended exposure limit of 10 ppm.[1,2] H_2S is also an intrinsic gasotransmitter that is involved in neural and cardiovascular systems[3] with potential therapeutic applications.[4] This potent biological activity is possible because H_2S crosses cell membranes readily. In contrast to molecules like water, where passage is facilitated by aquaporins,[2] no facilitator is needed for H_2S permeation; experiments by Mathai et al.[5] determined that the permeability coefficient of H_2S through a lipid bilayer is at least 0.5 cm/s, which is 4 orders of magnitude higher than that of H_2O. This degree of permeability is comparable to those of nonpolar molecules like O_2 and CO_2,[6] despite the polarity and hydrogen-bonding capability of H_2S.

Molecular simulations have emerged as a powerful tool for understanding membrane permeability. The solubility–diffusion model provides a straightforward strategy for calculating the permeability coefficient of a solute (P).[7] In this model, P can be expressed as a function of the Gibbs energy ($\Delta G(Z)$)[8] and diffusion coefficient ($D(Z)$) of the solute along the transmembrane axis (Z). These properties are calculated along this coordinate from restrained molecular dynamics (MD) simulations. An integral along the axes spanning the membrane (z_1 and z_2) provides P (eq 1). To determine the origin of its high permeability, we computed the permeability of H_2S using MD simulations. For comparison, we also computed the permeability of H_2O.

$$\frac{1}{P} = \int_{z_1}^{z_2} \frac{\exp(\Delta G(Z)/k_B T)}{D(Z)}\, dZ \qquad (1)$$

Permeability calculations require accurate molecular models of the solute, bilayer, and surrounding solution. Many conventional models neglect the effect of induced polarization, which is significant in these simulations because the solutes move from a polar aqueous solution across the nonpolar membrane interior. The Drude polarizable model was used in this study because it is possible to perform molecular dynamics simulations of large systems efficiently[9] and parameters have been developed for H_2O,[10] H_2S,[11,12] and DPPC lipids.[13] This model incorporates the effect of induced polarization, so the change in polarization of the solute during the permeation process is included rigorously. The Drude force field was also developed so that diffusion coefficients calculated with it are accurate. For example, the TIP3P water model that is commonly used with nonpolarizable lipid models predicts a self-diffusion coefficient of 5.3×10^{-5} cm^2/s, which is more than double the experimental value of 2.30×10^{-5} cm^2/s. In comparison, the SWM4-NDP Drude water model used in this study is in excellent agreement, predicting a value of 2.33×10^{-5} cm^2/s.[10]

The model used in these simulations was a planar bilayer of 132 DPPC lipids surrounded by 8538 water molecules in an orthorhombic simulation cell (63 Å × 63 Å × 105 Å).[14] The simulations were performed in the isothermal–isobaric ensemble with a temperature of 298.15 K and a pressure of 1.0135 bar, corresponding to the experimental conditions of the permeability measurements. We note that although this temperature is below the experimental melting temperature of 314 K for a DPPC bilayer, the bilayer remained fluid in all of the simulations. The full details of our model and simulations are included in the Supporting Information.

The Gibbs energy profile $\Delta G(Z)$ was calculated by an umbrella sampling simulation.[15] Neale et al.[16] showed that transmembrane Gibbs energy profile calculations are sensitive to the initial configuration and require very long simulations to reach convergence. To address this, two independent simulations were performed for each solute, sampling a total of 2 μs of MD for each profile. The diffusion coefficient profile was calculated from a second set of simulations using the autocorrelation function of a harmonically restrained solute.[17] The profiles are discussed in terms the regions defined by Marrink and Berendsen:[7]

- region 1: lipid tail ends (Z < 5 Å)
- region 2: lipid tails (5 Å < Z < 13 Å)
- region 3: headgroups (13 Å < Z < 20 Å)
- region 4: bulk water (Z > 20 Å)

The Z-dependent diffusion coefficients for the two solutes show significant variation across the bilayer (Figure 1a). The diffusion coefficient of H_2O is highest in the disordered lipid tail ends (region 1), where there are no hydrogen-bonding interactions to impede its movement. The diffusion coefficient of H_2S is lower at the center of the membrane than in solution, indicative of the higher effective viscosity of the lipid tails in

Received: August 6, 2014
Published: October 17, 2014

   dx.doi.org/10.1021/ja508063s | J. Am. Chem. Soc. 2014, 136, 15111–15113

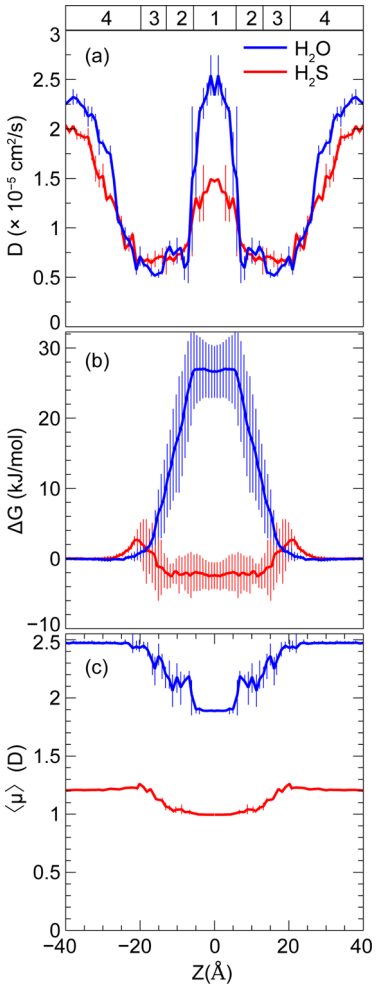

Figure 1. (a) Diffusion coefficient, (b) Gibbs energy, and (c) average solute dipole moment profiles for the permeation of H_2O and H_2S across a DPPC lipid bilayer. The Z axis is the difference in the center of mass of the bilayer and the solute. Profiles were averaged over both leaflets so that they are symmetric about $Z = 0$ Å.

comparison with water. The diffusion constants of both solutes decrease to ~1 × 10^{-5} cm^2/s in the tails and headgroups (regions 2 and 3). The diffusion coefficients are attenuated in the water layer at the membrane interface; both solutes only reach their bulk liquid values at ~15 Å above the water−bilayer interface. This is consistent with observations of changes in water dynamics at lipid bilayer interfaces.[18,19]

The Gibbs energy profiles of permeation for H_2O and H_2S show sharper differences (Figure 1b). The barrier for H_2O permeation reaches a maximum of 27 kJ/mol when H_2O is in the lipid tails (region 1), consistent with earlier simulations.[7,20] The Gibbs energy profile for H_2S permeation is much flatter; a small barrier of 2.6 kJ/mol occurs at the membrane−water interface, but the profile decreases and then plateaus at −2.5 kJ/mol in the lipid tails (regions 1 and 2).

These data were used to calculate the permeability coefficients of H_2O and H_2S using eq 1. The calculated and experimental values are presented in Table 1. The calculated value of 2.6 × 10^{-5} cm/s for the permeability of H_2O matches experiment exactly. This agreement is somewhat fortuitous because there is some variety in the reported experimental values and there are inherent limitations to the accuracy the solubility−diffusion model. In comparison, the permeability

Table 1. Experimental and Calculated Membrane Permeability Coefficients for H_2O and H_2S

	permeability coefficient (cm/s)	
solute	calcd	exptl
H_2O	(2.6 ± 0.5) × 10^{-5}	(2.6 ± 0.5) × 10^{-5} [a]
H_2S	11.9 ± 0.7	>0.5 ± 0.4[b]

[a]95% DPPC/5% DSPE-PEG2000 bilayer.[21] [b]Reconstituted bacterial membrane.[5]

coefficient at 50 °C calculated using the CHARMM27/TIP3P nonpolarizable force field is 1.3 × 10^{-3} cm/s.[22] The calculated permeability of H_2S is 11 cm/s, which is comparable to those of rapidly permeating gases like O_2. This implies that the lower bound of 0.5 cm/s determined experimentally by Mathai et al. may be a significant underestimate.

The dominant factor that allows H_2S to permeate much more rapidly than H_2O is its lower transmembrane Gibbs energy profile. These profiles can be understood on the basis of differences in solvation of the solutes in water and in hexadecane, a model for the lipid tail region at the center of the bilayer. These energies were calculated using free energy perturbation[23] and are collected in Table 2. For both solutes,

Table 2. Calculated Solvation Energies (in kJ/mol) of H_2O and H_2S in Water and Hexadecane (hex); The Rows Indicated by Δ Show the Water−Hexadecane Transfer Energies

solute	solvent	ΔG_{elec}	ΔG_{disp}	ΔG_{rep}	ΔG_{tot}
H_2O	water	−33.2	−13.8	23.5	−23.5
	hex	−3.2	−13.2	15.8	−0.6
	Δ	30.0	0.6	−7.7	22.9
H_2S	water	−3.9	−29.6	31.6	−2.0
	hex	−0.5	−27.2	21.6	−6.0
	Δ	3.4	2.4	−10.0	−4.0

the dispersion components (ΔG_{disp}) in the two solvents are roughly equal. The repulsive components (ΔG_{rep}) for both solutes are larger in water because of its stronger cohesive forces, creating a small thermodynamic driving force for the solutes to transfer to hexadecane. The largest difference occurs in the electrostatic component: H_2O has strong hydrogen-bonding interactions with water that are absent in hexadecane, so this component disfavors transfer of H_2O from water to hexadecane by 30.0 kJ/mol. The electrostatic component of H_2S solvation in water is relatively small (ΔG_{elec} = −3.9 kJ/mol) because its large van der Waals radius and modest dipole moment preclude strong hydrogen-bonding interactions with water.[12] This weakly hydrophobic solvation causes H_2S to be roughly equally soluble in water or the paraffinic interior of the bilayer, consistent with its relatively large experimental partition coefficients with nonpolar solvents like hexadecane,[24] *n*-octanol, hexane, and DPLC liposome bilayers.[25]

This correlation between the high permeability of H_2S and its tendency to partition into the nonpolar interior of the membrane is consistent with Overton's rule, which predicts that hydrophobic molecules will permeate more quickly.[26] This rule was quantified by Walter and Gutknecht,[27] who showed a very high correlation between the permeation coefficient and the water/hexadecane partition coefficient ($K_{hex/wat}$) for a set of small molecules. Figure 2 shows the relation between the permeabilities and partition coefficients for the molecules

dx.doi.org/10.1021/ja508063s | J. Am. Chem. Soc. 2014, 136, 15111−15113

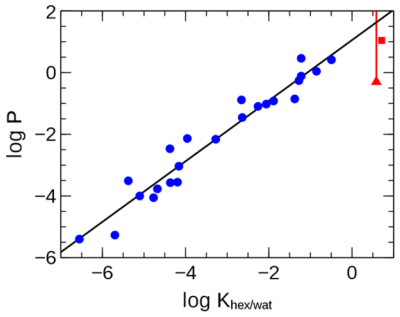

Figure 2. Log–log plot of experimental permeability (P) vs water/hexadecane partition coefficient ($K_{hex/wat}$) for small-molecule solutes (blue) and experimental and calculated values for H_2S (red). The red triangle and line correspond to the lower bound determined experimentally. The red square corresponds to the value calculated in this work.

reported by Walter and Gutknecht and for the experimental and calculated data for H_2S. The $K_{hex/wat}$ of H_2S is consistent with the high calculated permeability.

The average dipole moments of the solutes decrease when they move from solution to the membrane interior (Figure 1c). At the center of the membrane, the average dipole moments of the solutes are equal to their values in the gas phase, indicating that they do not experience any significant induced polarization. H_2O experiences a large decrease, from 2.5 to 1.9 D, because of the loss of polarizing hydrogen-bonding interactions. Although H_2S is more polarizable than H_2O,[28] it experiences a smaller change in average dipole moment; its dipole moment decreases from 1.2 to 1.0 D. H_2S is only weakly polarized in water because it is solvated like a hydrophobic solute, without strong hydrogen-bonding interactions with water.[12]

In conclusion, the simulations performed in this study provide a simple explanation for the high membrane permeability of H_2S. On the basis of the solubility–diffusion model, the permeability coefficients of H_2S and H_2O were calculated using an all-atom polarizable model and are in good agreement with the experimental values. Although the diffusion coefficient profile of H_2S is systematically lower than that of H_2O, the differences in the transmembrane Gibbs energy profiles are more dominant. H_2S experiences essentially no barrier to permeation because it is hydrophobic, so it can partition into the paraffinic interior of the membrane readily. This ability to pass through lipid bilayers freely helps explain both the broad toxicity of H_2S and its ability to serve as a signaling molecule.

■ ASSOCIATED CONTENT

Supporting Information

Computational details, modifications to the NAMD source code, and sample input files. This material is available free of charge via the Internet at http://pubs.acs.org.

■ AUTHOR INFORMATION

Corresponding Author

crowley@mun.ca

Notes

The authors declare no competing financial interest.

■ ACKNOWLEDGMENTS

We thank NSERC of Canada for funding through a Discovery Grant (Application 418505-2012) and the Research and Development Corporation of Newfoundland and Labrador for an Ignite R&D Grant. We thank Tiffany Tozer for proofreading the manuscript. Computational resources were provided by the Compute Canada Consortium (CCI: djk-615-ac).

■ REFERENCES

(1) Beauchamp, R. O.; Bus, J. S.; Popp, J. A.; Boreiko, C. J.; Andjelkovich, D. A.; Leber, P. *Crit. Rev. Toxicol.* **1984**, *13*, 25.
(2) Carbrey, J.; Agre, P. *Handb. Exp. Pharmacol.* **2009**, *190*, 3.
(3) Gadalla, M. M.; Snyder, S. H. *J. Neurochem.* **2010**, *113*, 14.
(4) Szabo, C. *Nat. Rev. Drug Discovery* **2007**, *6*, 917.
(5) Mathai, J. C.; Missner, A.; Kügler, P.; Saparov, S. M.; Zeidel, M. L.; Lee, J. K.; Pohl, P. *Proc. Natl. Acad. Sci. U.S.A.* **2009**, *106*, 16633.
(6) Subczynski, W. K.; Hyde, J. S.; Kusumi, A. *Proc. Natl. Acad. Sci. U.S.A.* **1989**, *86*, 4474. Missner, A.; Kügler, P.; Saparov, S. M.; Sommer, K.; Mathai, J. C.; Zeidel, M. L.; Pohl, P. *J. Biol. Chem.* **2008**, *283*, 25340.
(7) Marrink, S.-J.; Berendsen, H. J. C. *J. Phys. Chem.* **1994**, *98*, 4155.
(8) The Gibbs energy profile also called the potential of mean force (PMF).
(9) Jiang, W.; Hardy, D. J.; Phillips, J. C.; MacKerell, A. D.; Schulten, K.; Roux, B. *J. Phys. Chem. Lett.* **2011**, *2*, 87.
(10) Lamoureux, G.; Harder, E.; Vorobyov, I. V.; Roux, B.; MacKerell, A. D., Jr. *Chem. Phys. Lett.* **2006**, *418*, 245.
(11) Riahi, S.; Rowley, C. N. *J. Phys. Chem. B* **2013**, *117*, 5222.
(12) Riahi, S.; Rowley, C. N. *J. Phys. Chem. B* **2014**, *118*, 1373.
(13) Chowdhary, J.; Harder, E.; Lopes, P. E. M.; Huang, L.; MacKerell, A. D., Jr.; Roux, B. *J. Phys. Chem. B* **2013**, *117*, 9142.
(14) The average lipid headgroup area in our simulations was ~59 Å^2, which is an underestimate of the experimental headgroup area of 64 Å^2 at 314 K. This discrepancy is inherent to the current version of the Drude lipid model and the lower simulation temperature.
(15) Torrie, G. M.; Valleau, J. P. *J. Comput. Phys.* **1977**, *23*, 187. Roux, B. *Comput. Phys. Commun.* **1995**, *91*, 275.
(16) Neale, C.; Bennett, W. F. D.; Tieleman, D. P.; Pomès, R. *J. Chem. Theory Comput.* **2011**, *7*, 4175.
(17) Woolf, T. B.; Roux, B. *J. Am. Chem. Soc.* **1994**, *116*, 5916. Hummer, G. *New J. Phys.* **2005**, *7*, 34.
(18) Fukuma, T.; Higgins, M. J.; Jarvis, S. P. *Biophys. J.* **2007**, *92*, 3603.
(19) Berkowitz, M. L.; Vácha, R. *Acc. Chem. Res.* **2012**, *45*, 74.
(20) Comer, J.; Schulten, K.; Chipot, C. *J. Chem. Theory Comput.* **2014**, *10*, 554.
(21) Terreno, E.; Sanino, A.; Carrera, C.; Castelli, D. D.; Giovenzana, G. B.; Lombardi, A.; Mazzon, R.; Milone, L.; Visigalli, M.; Aime, S. *J. Inorg. Biochem.* **2008**, *102*, 1112.
(22) Bemporad, D.; Essex, J. W.; Luttmann, C. *J. Phys. Chem. B* **2004**, *108*, 4875.
(23) Deng, Y.; Roux, B. *J. Phys. Chem. B* **2004**, *108*, 16567.
(24) Clarke, E. C. W.; Glew, D. N. *Can. J. Chem.* **1971**, *49*, 691. King, M. B.; Al-Najjar, H. *Chem. Eng. Sci.* **1977**, *32*, 1241.
(25) Cuevasanta, E.; Denicola, A.; Alvarez, B.; Möller, M. N. *PLoS One* **2012**, *7*, No. e34562.
(26) Missner, A.; Pohl, P. *ChemPhysChem* **2009**, *10*, 1405.
(27) Walter, A.; Gutknecht, J. *J. Membr. Biol.* **1986**, *90*, 207.
(28) The gas-phase polarizabilities of H_2S and H_2O are 3.63 and 1.44 Å^3, respectively, but the liquid-phase Drude model polarizabilities are 2.5 and 0.97 Å^3, respectively.